Submicron Trenches Reduce the *Pseudomonas fluorescens* Colonization Rate on Solid Surfaces

Carolina Díaz,[†] Patricia L. Schilardi,[†] Paula C. dos Santos Claro,[†] Roberto C. Salvarezza,[†] and Mónica A. Fernández Lorenzo de Mele*[,†,‡]

Instituto de Investigaciones Fisicoquímicas Teóricas y Aplicadas (INIFTA), Facultad de Ciencias Exactas, Universidad Nacional de La Plata-CONICET, Casilla de Correo 16, Sucursal 4, (1900) La Plata, Argentina, and Facultad de Ingeniería, Universidad Nacional de La Plata, La Plata, Argentina

ABSTRACT Bacterial adhesion and spreading on biomaterials are considered key features of pathogenicity. Roughness and topography of the substrate have been reported to affect bacterial adhesion, but little is known about their effect on spreading. Submicron row and channel tuning with bacterial diameter (S2) were designed to test bacterial motility on these surfaces. Random nanometer-sized structures (S1) were used as controls. Optical microscopy and AFM were employed to detect biological and surface pattern details in the micro- and nanoscale, respectively. Results showed that motility strategies (flagella orientation, elongation, aggregation in rafts, formation of network structures, and development of a bacterial frontier) were affected by the presence of submicropatterns. Importantly, the rate of bacterial spreading on S2 was significantly reduced and influenced by the orientation of the submicropatterns. Consequently, submicroengineered substrates could be employed as a tool to downgrade bacterial colonization. Such patterns could impact on the design of proper engineered structures to control biofilm spreading on solid surfaces.

KEYWORDS: Cell adhesion • AFM • cell recognition • nanotechnology • bacterial colonization • bacterial adhesion • biofilm • nanotopography • micropatterning • microstructure

1. INTRODUCTION

Biomaterial implant-related infections remain as one of the main causes of implant failures. Bacteria that cause these infections are difficult to eradicate because they live in biofilms (1). The principal implants that deal with biofilm-associated infections are (2) central venous catheters, heart valves, ventricular assist devices, coronary stents, neurosurgical ventricular shunts, implantable neurological stimulators, arthro-prostheses, fracture-fixation devices, and inflatable penile implants. A successful strategy to inhibit biofilm formation and spreading might be a valuable way to inhibit this dangerous process. Thus, one of the most important challenges in the biomaterials field is the development of materials with specific surface properties that avoid bacterial colonization in order to prevent infections.

During surface colonization bacteria display different forms of motility, including swimming, twitching, gliding, and swarming. Bacterial migration is influential on several pathogen−host interactions in plants and animals. Motility facilitates ascending colonization of the urinary tract by bacteria yielding to biofilm formation in catheters (3, 4) as well as migration in soil environments (5). Swarming is the fastest mode of surface social translocation characterized by cooperative movement of bacteria that migrate above the solid substrate in groups. According to studies made on agar surfaces, swarming is strictly dependent on the ability of bacteria to undergo a differentiation process distinguished by the production of specialized swarmer cells longer and sometimes more flagellated than the swimming cells (6, 7). Swarmer differentiation is also associated with bacterial antibiotic resistance to a variety of structurally and functionally different compounds (8−10).

Pseudomonad biofilms have marked impact on medical, environmental and industrial fields. They are frequently used as model species for studying social motility of bacteria on solid surfaces (8−20). In concordance with other bacterial biofilms, *Pseudomonad* biofilms are more resistant to antibiotics than single planktonic cells (21). *Pseudomonas fluorescens* (*P. fluorescens*), closely related to two other members of the fluorescent *Pseudomonad* group, *P. putida* and *P. aeruginosa*, was employed in this work.

Unfortunately, only a few studies have been made in relation to *Pseudomonad* motility on solid surfaces. Phase, dark field, and computer-enhanced microscopy were used to observe *P. fluorescens* colonization on transparent solid substratum (22). The authors described that, initially, cells were freely motile, performing circular loop movements within the plane of the solid−liquid interface. Subsequently, cells attached apically and rotated. This type of attachment was reversible. Then, the positions of the cells changed and finally they were longitudinally attached and increased in length. After 1 h exposure cells divided (doubling time 1.2 h),

* To whom correspondence should be addressed. Tel: 54 221 4257430/7291. Fax: 54 221 4254642. E-mail: mmele@inifta.unlp.edu.ar; fernandezlorenzom@hotmail.com.

Received for review September 23, 2008 and accepted December 8, 2008

[†] Instituto de Investigaciones Fisicoquímicas Teóricas y Aplicadas (INIFTA), Facultad de Ciencias Exactas.

[‡] Facultad de Ingeniería.

DOI: 10.1021/am8000677

Published on Web 01/09/2009

separated, and moved apart laterally, to lay parallel within the same plane. The instability of the group was observed after 4 h exposure when emigration of some cells occurred. The authors also described the shifting and sliding of the groups of cells as a "packing maneuver", though the mechanism was unknown. Surface motility is a major trait for competitive colonization of vegetables by *Pseudomonas fluorescens* (23, 24). The motile strain attached about 4 times more rapidly and achieved higher final cell density on surfaces than did the nonmotile strain.

The aim of this paper is to assess opaque submicropatterned surfaces that are in tune with bacterial diameter and investigate if they affect bacterial strategies to move and reduce their colonization rate. In a previous work (25) we showed that AFM is suitable to sense bacterial organelles "in situ" and their distribution on metallic surfaces, avoiding the removal of the biological material from the substratum frequently required in the case of transmission electron microscopy (TEM). We have taken advantage of high-resolution atomic force microscopy (AFM) images to detect biological details in the nanoscale that cannot be sensed by using other techniques such as video microscopy.

We have chosen gold as the model material because of its biocompatibility, malleability, and resistance to corrosion, especially in biological media. In this way the influence of submicrostructures could be analyzed without the interference of corrosion products and/or toxicity of metal ions associated with metal corrosion. Importantly, gold is highly opaque to X-rays, aiding positioning of wires and small devices. Currently, there are several direct applications of gold in medical devices, which include dental applications, wire for pacemakers, and gold-plated stents. Additionally, gold-plated myringotomy tubes are used for implantation in the tympanic membrane to drain and temporarily aerate the tympanic cavity (26).

2. MATERIALS AND METHODS

Two gold substrates with different submicron surface structures were used. The first substrate was a polycrystalline continuous gold film (S1) prepared by physical vapor deposition of a 200 nm gold layer on a glass substrate covered by a thin Cr layer (Arrandee, Germany). The surface exhibited a random nanometer-sized structure consisting of 50−100 nm grains. The grains introduced a typical wavelength of about 100−200 nm. Typical values of the root-mean-square roughness (w) measured on 10 μm^2 AFM images were $w = 2-3$ nm. The absence of surface contamination was checked by X-ray photoelectronic spectroscopy (XPS). A typical spectrum (Supporting Information, Figure 1-S) showed only small amounts of carbon and oxygen, as expected for substrates exposed to air. The second substrate (S2) was submicrostructured gold prepared by combining physical vapor deposition (PVD) with molding and replication techniques as described elsewhere (27). Basically, the strategy consists of covering a nano-/microstructured master with a self-assembled monolayer (SAM) and the subsequent deposition of a gold film. Because of the antiadherent properties of the SAM, the gold film is easily detached from the master and the inner face of the film is a mold of the master. In this work we used a copper mold covered with a dodecanethiol SAM. Gold was deposited on the mold by PVD and after detachment was used as substrate to investigate bacterial colonization. The face of the substrate to be exposed to the culture was peeled immediately before the assays. This procedure provides a clean gold surface without contamination from the SAM (28). The substrate consisted of a grid of 550 nm wide gold rows separated by channels of 750 nm width and 120 nm depth. The wavelength and amplitude were 1.3 μm and 120 nm, respectively. In this case the w value (from 10 × 10 μm^2 AFM images) was 40 nm. The size of the trenches tuned very well with bacteria diameter. Occasionally, hexagonal gold patterns (12 μm apothem separated by 7 μm width channels) prepared by stencil lithography were used for testing bacteria adhesion.

P. fluorescens strain, kindly provided by Dr. Christine Gaylarde (Department of Biology and Chemistry, UNIJUI, RS, Brazil), was identified by standard bacteriological tests using selective growth media and biochemical tests. This strain was maintained as an inoculated slant in cetrimide agar (DIFCO) at 28 °C. This slant was incubated under conditions for microbial growth and then stored in a refrigerator at a temperature below the minimum required for culture growth. Passages of the stock were made every 20 days.

The inoculum was prepared by suspending a cetrimide agar slant (24 h old) in 2 mL of sterile nutrient broth for microbiology (Merck). The typical composition is peptone from meat (5.0 g/L) and meat extract (3.0 g/L). The pH of this medium is 7 ± 0.2 at 25 °C. The inoculum was poured into an Erlenmeyer flask containing 300 mL of nutrient broth medium and the mixture kept on a rotary shaker for 3 h at 28 °C. After 24 h growth, the different substrates were placed into the culture so that a bacterial biofilm could form on them. Thus, all substrates were exposed at the same time to the same culture. In order to study the social motility of *P. fluorescens* on S1 and S2 substrates without the interference of planktonic cells in the biofilm spreading, half of the S1 and S2 surfaces was masked with an inert material (Teflon ribbon) in order to avoid bacterial attachment onto this area. Then the substrates were placed into a 24 h *P. fluorescens* culture, and after 30 min they were removed and washed with double-distilled sterile water in order to remove those cells which were not tightly attached to the surface. Subsequently, the masks were removed from the surface and the entire substrates were immersed in sterile nutrient broth medium for different times (10 min, 30 min, 1 h, and 2 h). Under these conditions the attached bacteria moved to colonize the bare area that had been previously masked. The S2 substrates were immersed in the cultured medium inoculated with *P. fluorescens* exhibiting two orientations: with the trenches parallel to (S2Pa) and perpendicular to (S2Pe) the direction of the advance of the biofilm.

During the assays S1 and S2 were immersed simultaneously (in the same culture medium and under identical conditions) and the biological responses to the topographical variation of the surfaces, as the unique variable, were compared. After the immersion period, the substrates were removed, gently washed with double-distilled sterile water, and dried in air. The assays were repeated three times, and results were statistically analyzed. Similar statistically significant differences were found between S1 and S2 substrates for the different assays.

The samples were imaged by AFM (Nanoscope IIIa, Digital Instruments) operating in contact mode using silicon nitride tips and by optical microscopy (Olympus BX51). Observations of the stained samples through epifluorescent microscopy were also made.

3. RESULTS AND DISCUSSION

We will describe the present results in the context of the initial stages of biofilm spreading on solid surfaces immersed in sterile medium: i.e., avoiding the interference of planktonic cells. Bacterial behavior at this scene and the interactions of the microorganisms with the solid surfaces will be

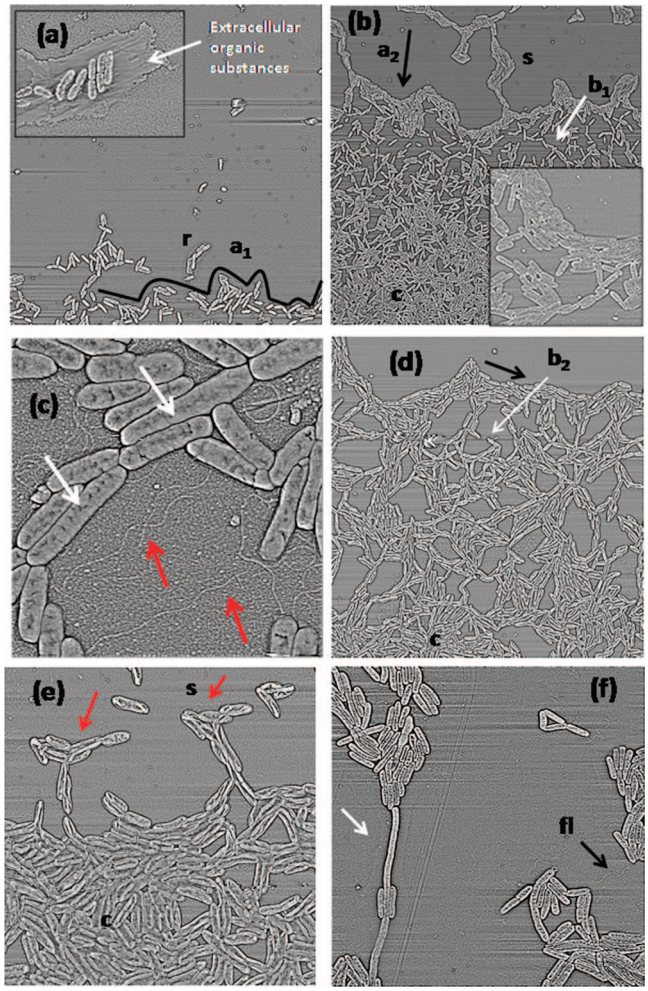

FIGURE 1. AFM images of early stages of bacterial spreading on an S1 surface immersed in sterile culture medium: (a) 75 × 75 μm^2 (high-pass filtered) of the bacterial front on S1 after 10 min bacterial spreading (the black line indicates the early bacterial front, and the inset shows extracellular organic substances); (b) 100 × 100 μm^2 (high-pass filtered) after 30 min bacterial spreading (the inset shows a detail of the front); (c) 10 × 10 μm^2, detail of the center of Figure 2b showing bacterial organization behind the front (the white arrows indicate elongated bacteria and the red arrows flagella connecting the neighboring cells); (d) 60 × 60 μm^2 (high-pass filtered) of S1 colonization after 2 h bacterial spreading (the black arrow indicates the direction advance of the bacteria at the front); (e) 24 × 24 μm^2 initial stages of spearhead arrangements (red arrows); (f) 30 × 30 μm^2 image showing bacterial elongation to form a "bridge" between bacterial groups. Legend: a_1, a_2, bacterial front; b_1, b_2, open spreading areas; c, condensed spreading area; fl, flagellum; r, raft; s, spearhead.

analyzed first at random (S1) and then on the patterned S2Pa submicrostructured surfaces. Finally, bacterial spreading on S2Pa and S2Pe, characterized by different orientations of the trenches (parallel or perpendicular) in relation to the direction of bacterial advance, will be compared. The processes occurring at the interface in the submicroscale by were observed by AFM and compared in order to characterize the migration process on each surface. Results of global bacterial spreading on the surface made by optical microscopy are also presented.

Bacterial Colonization of S1. Figure 1a shows the appearance of the substrate after the removal of the mask and subsequent exposure to the sterile culture medium for 10 min. The first steps of organization of a typical bacterial front invading the bare area of a random nanostructured gold surface (S1) can be observed. At this early stage of migration, bacteria form open and ramified patterns usually 1 or 2 bacteria wide. In the absence of planktonic microorganisms, bacterial spreading can essentially be attributed to the result of bacterial motility. A primitive structure (a_1 in Figure 1a) may be interpreted as the very early step of bacterial front formation. The first attempt of organization in small rafts (r in Figure 1a) also takes place during this period.

The inset in Figure 1a shows that the surface beneath the bacterial raft and its surroundings is covered by organic substances, probably extracellular polymeric substances and surfactants. The production of these substances and the association of cells in groups may facilitate movement and save energy by reducing the bacterial surface in contact with the aqueous medium, diminishing the frictional resistance. On movement as a group, higher average velocities are reached with the consequent advantage of reducing colonization time.

A more defined bacterial frontier with the typical structure of swarming spreading was observed on S1 after 30 min exposure (a_2 in Figure 1b). The bacterial front, consisting of a 2−10 microorganisms wide line, ran perpendicularly to the direction of bacterial advance (see the inset of Figure 1b) and formed a clear limit for several hundreds of bacteria that were moving out of the original colonization limit on the substrate. This well-defined undulating edge impeded the escape of the inner cells at the back and forced the aggregation process. This picture indicates that our results at the metal/liquid interface are similar to those found at agar−air interfaces after inoculation in the center of the Petri dish (9, 29, 30). Frequently, multiple spearhead rafts emerged at various points along the advancing front (s in Figure 1b).

A careful analysis of Figure 1a−d shows a sequence of the different stages of the self-engineered spatial organization process. The advance of the front left bare areas behind it that were occupied by single cells (b_1 in Figure 1b). These spearheads can meander and merge with other groups, leading to the formation of a network of trails after 2 h (b_2 in Figure 1d). Again, similar results were previously reported for other microorganism/substrate systems at the air−agar interface (31). AFM images show that these single cells contacted the others by flagella and joined them, forming rafts of parallel cells (Figure 1c,f) that gathered together forming nets (b_2 in Figure 2d). It has been reported that this process is probably assisted by chemical signals (19). When the rafts of the net aggregated, forming a compact film (c in Figure 1d), some fresh branches escaped from the aligned front, forming new spearheads (s in Figure 1e) that moved out following the direction of bacteria displacement to explore the uncovered substrate (r in Figure 1a). The presence of flagella (fl in Figure 1f) not only favored motility of the aggregates but also suggests, as for the case of single cells, cell to cell communication to underlie the continuous cell aggregation (9, 19).

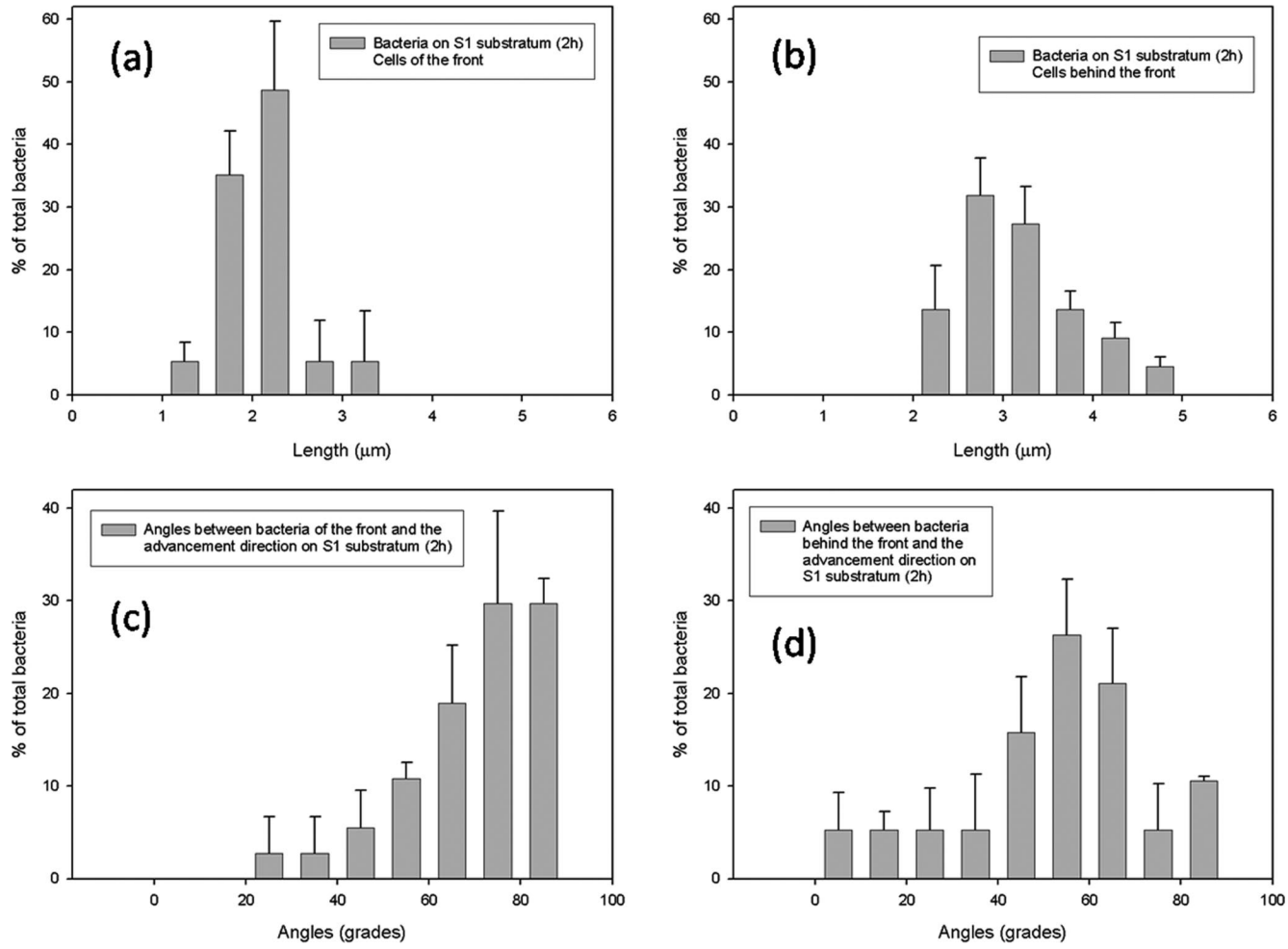

FIGURE 2. Histograms showing distributions of bacterial length (a and b) and orientation (c and d) after 30 min spreading on S1: (a, c) at the front and (b,d) behind the front (high-pass filtered). Data were obtained from AFM images.

Table 1. Average Bacterial Length on S1 Surfaces

position	av length (μm)[a]
front bacteria	2.15 ± 0.35
bacteria behind the front	3.21 ± 0.57

[a] Significantly different ($p < 0.05$).

The analysis of the lengths (Figure 2a) and orientation (Figure 2b) of the cells showed that 87% of the cells behind the front are longer than 2.5 μm and more than 10% are longer than 4 μm. In contrast, only 10% of the front cells are longer than 2.5 μm (Figure 2a). Table 1 shows the average length of the cells according to their position (in the front or behind it). Considering that the average length of planktonic cells is 1.86 ± 0.6 μm (25), the cells behind the front (average length: 3.21 μm) were significantly ($P < 0.05$) longer than planktonic cells. Figure 1c,f (white arrows) shows that elongation may be another strategy to contact cells and other aggregates in order to gather the organized mobile groups. In fact, elongation was only previously described for raft formation as a differentiation process useful for the alignment that facilitates the contact of the cells (3, 7). To bring this about, bacteria suppress cell division and become elongated. Upon elongation some cells alter their collective movement from the typical run and tumble of the short cells to a coordinated forward–backward movement, which yields organized branches (29, 31). Importantly, the present results show novel evidence suggesting that elongation can also be used as a "bridge" strategy to join small groups of cells. In agreement, the inner part of the net consisted of rafts connected by narrow ramified structures frequently containing elongated bacteria.

As was mentioned earlier, the external boundary remains aligned perpendicularly to the direction of the advance (a_2 and inset in Figure 1b and black arrow in Figure 1d). Figure 2c shows that more than 70% of these cells in this region are nearly perpendicular to the direction of the spreading, forming a clear frontier for the global expansion. This preferential orientation was not observed at the back of the front (Figure 2d).

Considering that *P. fluorescens* doubling time on solid surfaces is 1.2 h, experiments with 10 min, 30 min, and 1 h immersion times should mainly describe bacterial motility on the surface with no significant influence of bacterial growth. In addition, the effect of planktonic cells released from the biofilm on bacterial attachment should be minimum, taking into account that this process has been previously described after 4 h exposure (22) for *P. fluorescens* and 5 h for other *Pseudomonads* (32).

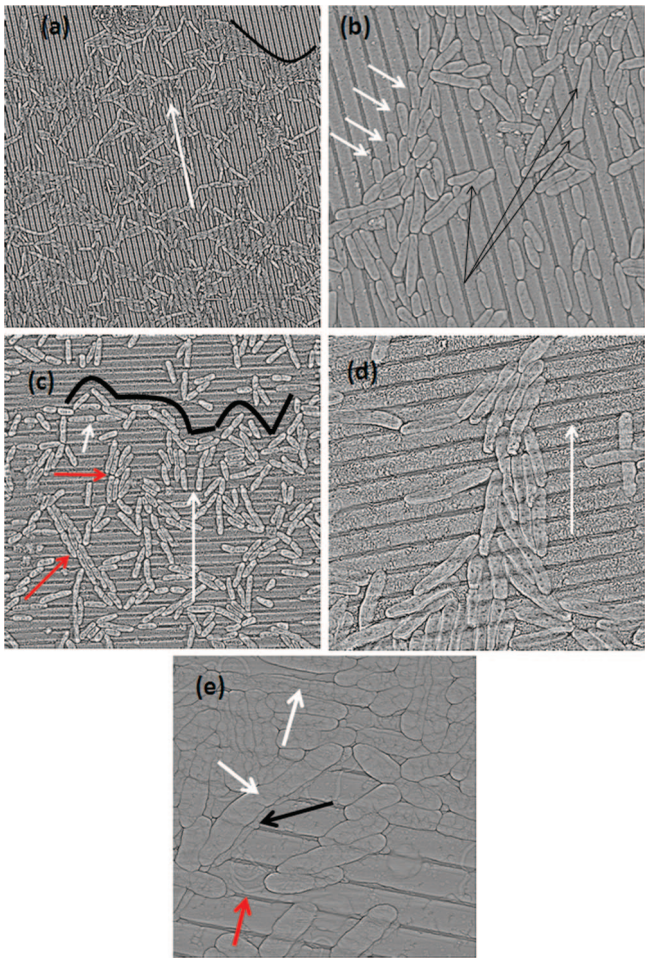

FIGURE 3. AFM images of the bacterial front on S2 surfaces immersed in sterile culture medium: (a) 80 × 80 μm^2 (high-pass filtered) bacterial front after 1 h spreading on S2Pa (the white arrow indicates the direction of advance; preliminary attempts to form a front are shown with a black line); (b) 25 × 25 μm^2 (S2Pa) (white arrows indicate trapped cells that seem to be pushed by oblique cells, and black arrows point out elongated cells); (c) 40 × 40 μm^2 (S2Pe) (preliminary attempts to form a front are shown with a black line, and red arrows show small aggregates of parallel cells; the short white arrow shows bacteria trapped inside the trenches and the long white arrow the direction of the advance); (d) 20 × 20 μm^2 S2Pe (high-pass filtered) (bacteria trapped within the trenches seem to be pushed by those moving perpendicularly to the trenches; the white arrow shows the direction of the advancement); (e) 10 × 10 μm^2 (high-pass filtered) (white arrows indicate elongated bacteria; the black arrow shows the EPS underneath the cell, and the red arrow indicates flagella that are connecting neighboring bacteria).

Bacterial Colonization of S2. In the next section, the effect of the submicropattern (S2Pa substrate, with rows separated by channels of 120 nm depth and 750 nm width parallel to the direction of the advance) on the bacterial motility are described and discussed. The bacterial front on the S2Pa structure was completely disorganized after 10 and 30 min (not shown). The social motility with organized rafts was almost absent. Evidently, the processes involved in swarming were more difficult on S2 than on S1. Even for t = 2 h the front containing cells perpendicular to the cell advance was not well defined (Figure 3a) as in the case of S1 (a_2 and inset in Figure 1b). On S1 this front was characterized by highly motile cells which move in a parallel fashion to the spreading border. Quick movements were impeded on S2Pa surfaces due to the difficult displacement along this surface. Note that the rafts in Figure 3a,b for these long immersion times (2 h) are oriented obliquely to the trench direction. Following this orientation, bacteria avoided being trapped within the trenches. Some of the trapped bacteria seemed to be pushed by the oblique ones while trying to orient them in the direction of the angled advance (Figure 3b, white arrows). Elongated cells that join small cell groups can also be identified in Figure 3b (black arrows).

Now we will discuss the influence of the pattern orientation on bacterial size and distribution. The size and orientation of bacteria that spreaded on S2Pa and S2Pe are shown in Figure 4. It can be noticed that the bacterial length distribution was similar (Figure 4a,b). With respect to orientation, more than 35% of the bacteria were trapped or almost parallel (angle 0−19°) to the trench direction on S2Pa (Figure 4d). This orientation was not prevalent on S2Pe (Figure 4c). The average length of these bacteria was significantly smaller than that of the oblique species (Table 2). The critical role of the trench size in bacterial orientation and trapping was confirmed by using a different patterned substrate. We tested a gold substrate consisting of an array of hexagons (apothem 12 μm, height 145 nm) separated by trenches of 7 μm width (Supporting Information, Figure 2-S). In this case, some isolated bacteria and small groups (3−10 cells) randomly distributed on the micropatterned substrate were observed. No preferential trapping at the trenches or special orientation was evident from these images. In addition, in a previous report (25) we have demonstrated that features smaller (in the nanometer range) than the bacterial size are not efficient for preventing the formation of rafts in early stages of *P. fluorescens* adhesion. Therefore, it is evident that the best orientation and trapping can be obtained by using patterns that tune the bacteria size. These results are also important to discard the effect of capillary forces in ordering bacteria in the trenches, as ordering is observed only in the submicrometer-sized pattern.

Bacterial advance on S2Pa seemed to be directed according to 20−90° angles with respect to the trenches (Figure 4d). In fact, as mentioned above, the oblique movement of aggregates avoided bacterial trapping in the trenches. It seems that, after sticking to neighboring trapped isolated bacteria, the free oblique cells were able to push the confined ones outside the submicrofeatures. Consequently, an elevated energy demand to overcome the physical barrier of the walls was needed to move the trapped bacteria.

The formation of the front (perpendicular to the direction of the advance and consequently parallel to the trenches) was difficult on S2Pe because the cells may have been trapped in the trenches (Figure 3c). The advance on S2Pe (perpendicular to the trenches) seemed to be easier than on S2Pa (parallel to the trenches) and spearheads moved almost in a straight line (Figure 3d).

Comparison of the Colonizations on S1 and S2. The comparison of the bacterial surface coverage during the advance on S1 and S2 shown in Figure 5 (for different distances from the limit of the originally colonized area)

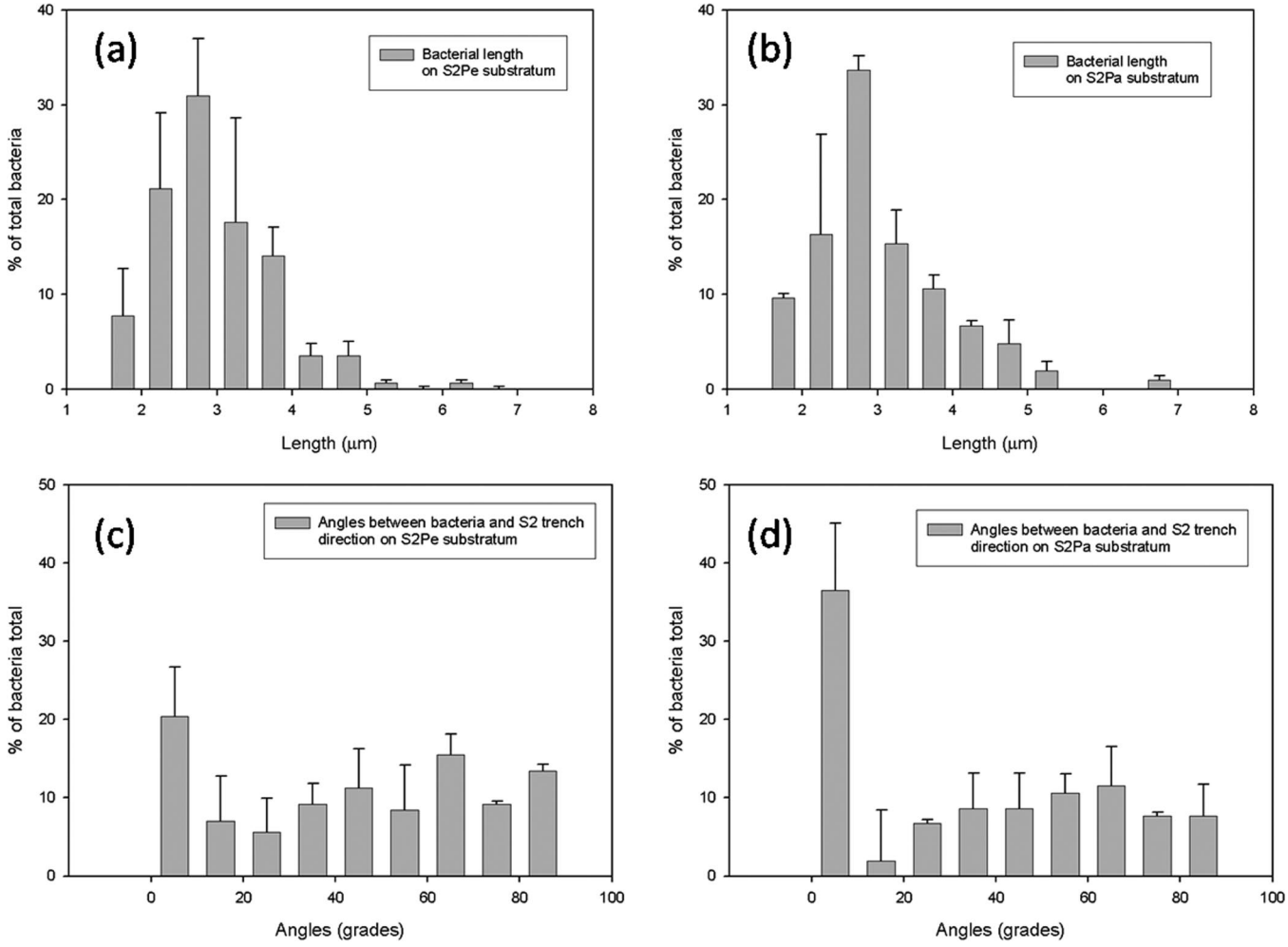

FIGURE 4. Distribution of bacterial length (a and b) and orientation (c and d) (angles with respect to the trench direction) on S2Pe and S2Pa. Values were measured on 40 × 40 μm^2 AFM images.

Table 2. Average bacterial length on S2 surfaces according to their orientation

	av length (μm)	
position	S2Pa	S2Pe[a]
parallel to the trench (direction 0−19°)	2.71 ± 0.71	2.75 ± 0.90
oblique to the trench (direction 20−90°)	3.13 ± 1.06	3.21 ± 0.76

[a] Significantly different ($p < 0.05$).

revealed a marked decrease of the colonized area on S2Pe in relation to S1. Similar results were obtained for S2Pa (not shown). It can be noticed that the coverage on S1 was almost 3-fold S2Pe coverage. These results suggest that twitching and social motility was hindered on S2 because bacteria had to defeat the S2 barriers that turned displacement very difficult. During twitching, isolated bacteria seem to have fallen within the 120 nm deep trenches due to jerky movements. If this were the case, the translocation should have been even more difficult for the trapped bacteria.

In Figure 3e (black arrow) it can be seen that EPS lifted up bacteria that were totally or partially within the trenches facilitating bacterial climb up the wall using the EPS "cushion" (25). Again, cell elongation (2 or 3 times the planktonic cell length) and duplication in order to reach and connect

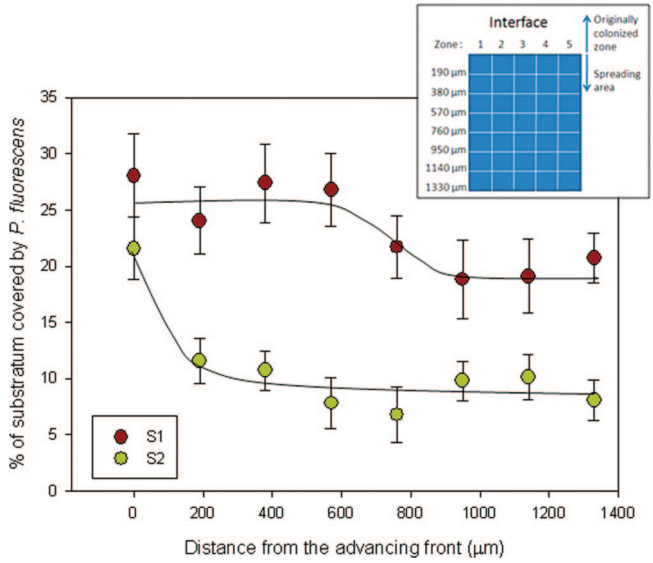

FIGURE 5. Average bacterial surface density on S1 (dark circles) and S2Pe (light circles) at different distances from the original bacterial front after 2 h spreading in sterile culture medium. The inset shows the different zones where attached bacteria were enumerated. Zones 1−5 are 304 μm wide.

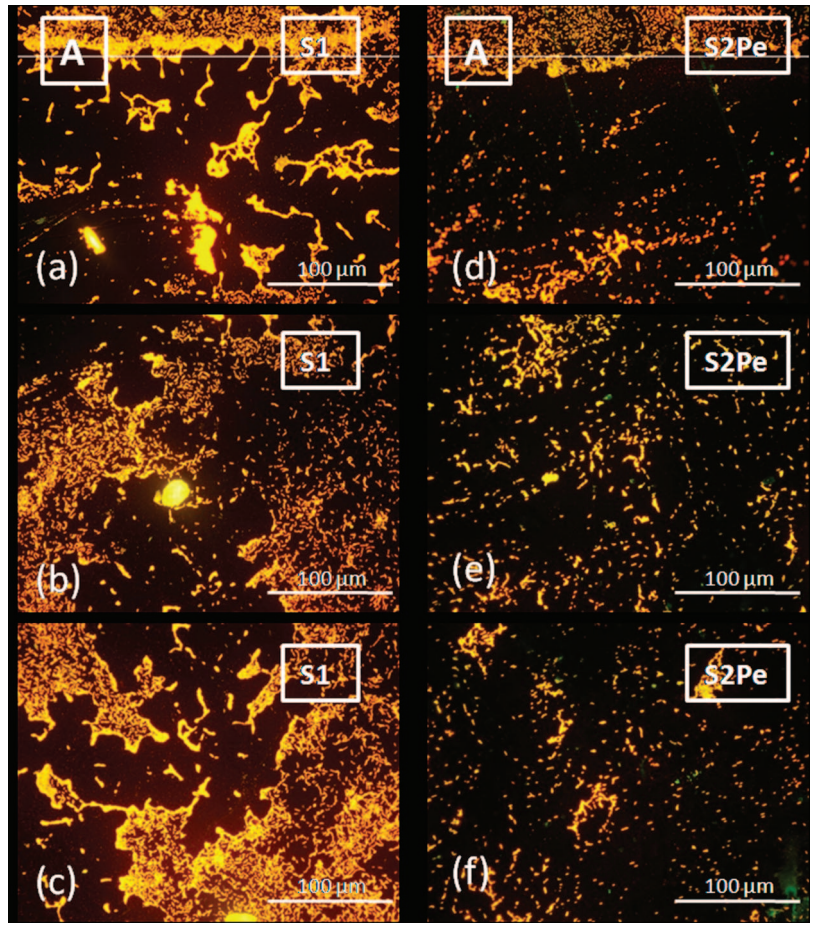

FIGURE 6. Optical micrographs of bacterial spreading on S1 (a−c) and S2Pe (d−f) after a 2 h immersion period in the sterile culture medium. The gray line and A indicate the original bacterial front (before the immersion in the sterile culture medium). The microphotographs show the images of the biofilm spreading at different distances (a and d, 197 μm; b and e, 435 μm; c and f, 673 μm) from the bacterial front.

the neighboring cells contributed to the confluence, as shown by the AFM image.

Optical microscopic observations revealed higher bacterial coverage on S1 than on S2Pa and S2Pe (Figure 6a−c). The long spearheads (2000 μm) formed on S1 surfaces (Figure 6c) seemed to glide easily through the surface. These large forefront aggregates were not found on S2, limiting the colonization capability. Consequently, optical microscopy observations also showed that the movement of bacteria on S2 surfaces was hindered by the submicropatterns, and, accordingly, the global rate of colonization on this surface was reduced.

According to Lawrence et al. (1986) (22) after 1 h exposure the cells attached on the glass divided, separated, and moved apart laterally, to lay parallel within the same plane. This type of movement on the transparent substrate that was described in detail by the authors was probably hindered in the case of S2 surfaces, impeding the sliding of the groups of cells.

By comparison of the bacterial advance on S1 and S2, we can speculate about the possible higher energy demand processes that make the motility on S2 trickier: higher production of extracellular polymeric substances to fill the trenches, "smoothing" the surface; higher work necessary to overcome the potential energy to climb up the wall of the trenches; hard work made by the bacteria outside the trenches to push those within them; energy lost because of friction of the bacterial body with a nonsmooth surface; difficult advance of a raft of bacteria with their bodies in different levels; difficult gathering of the groups and higher energetic demand of small groups moving independently.

5. CONCLUSIONS

The present results show that submicropatterns are influential on the strategies developed by bacteria to colonize metal surfaces immersed in aqueous media. The formation of rafts and networks, the elongation of cells, and the development of bacterial frontiers are some of these strategies. We provide evidence that self-engineering spatial organization of bacteria is conditioned by submicropatterns tuning with bacterial size (S2). Bacterial orientation and length are modified according to their position within the global spreading. Motility is trickier and probably requires higher energy on S2 than on S1. The orientation of the trenches also influences bacterial distribution and colonization strategies. Consequently, submicrostructure is one of the major factors affecting biofilm formation and spreading. Importantly, submicroengineered surfaces that tune with bacterial dimensions could be used as proper tools to hinder the bacterial colonization rate. The results are relevant

because of their promising impact on the design of suitable engineered structures to reduce/control biofilm spreading for industry, medicine, and environmental protection applications.

Acknowledgment. This work was supported by the ANPCyT (PICT 06-621, PICT 05-33225, PICT 05-32906, PAE 22771), UNLP (Projects 11/X425 and 11/I129), and CONICET. R.C.S. is a Guggenheim Fellow.

Supporting Information Available: Figures giving the X-ray photoelectron spectroscopy (XPS) spectrum showing small amounts of carbon and oxygen on S1 gold substrates used in this work, indicating that the surface was not contaminated by environmental organic compounds, and an AFM image of *P. fluorescens* attached to a micropatterned substrate after 2 h exposure to culture medium. This material is available free of charge via the Internet at http://pubs.acs.org.

REFERENCES AND NOTES

(1) McLean, R. J. C.; Whiteley, M.; Stickler, D. J.; Fuqua, W. C. *FEMS Microbiol. Lett.* **1997**, *154*, 259.
(2) Costerton, J. W.; Montanaro, L.; Arciola, C. R. *Int. J. Artif. Organs* **2005**, *28*, 1062.
(3) Allison, C.; Emody, L.; Coleman, N.; Hughes, C. *J. Infec. Dis.* **1994**, *169*, 1155.
(4) Stickler, D.; Morris, N.; Moreno, M. C.; Sabbuba, N. *Eur. J. Microbiol. Infect. Dis.* **1998**, *17*, 649.
(5) DeFlaun, M. F.; Tanzer, A. S.; McAteer, A. L.; Marshall, B.; Levy, S. T. *Appl. Environ. Microbiol.* **1990**, *56*, 112.
(6) Caiazza, N. C.; Shanks, R. M. Q.; O'Toole, G. A. *J. Bacteriol.* **2005**, *187*, 7351.
(7) Calvio, C.; Celandroni, F.; Ghelardi, E.; Amati, G.; Salvetti, S.; Ceciliani, F.; Galizzi, A.; Senesi, S. *J. Bacteriol.* **2005**, *187*, 5356.
(8) Doyle, T. B.; Hawkins, A. C.; McCarter, L. J. *J. Bacteriol.* **2004**, *186*, 6341.
(9) Köhler, T.; Kocjancic Curty, L.; Barja, F.; van Belden, C.; Pechére, J. C. *J. Bacteriol.* **2000**, *182*, 5990.
(10) Klausen, M.; Aaes-Jorgensen, A.; Molin, S.; Tolker-Nielsen, T. *Mol. Microbiol.* **2003**, *50*, 61.
(11) Landry, R. M.; Hupp, J. T.; Singh, P. K.; Parsek, M. R. *Mol. Microbiol.* **2006**, *59*, 142.
(12) Allesen-Holm, M.; Bundvig Barken, K.; Yang, L.; Klaussen, M.; Webb, J. S.; Kjelleberg, S.; Molin, S.; Givskov, M.; Tolker Nielsen, T. *Mol. Microbiol.* **2006**, *59*, 1114.
(13) Hsueh, P.-R.; Teng, L.-J.; Pan, H.-J.; Chen, Y.-C.; Sun, C.-C.; Ho, S.-W.; Luh, K.-T. *J. Clin. Microbiol.* **1998**, *36*, 2914.
(14) Pappas, G.; Karavasilis, V.; Christoul Tsianos, E. V. *Scand. J. Infect. Dis.* **2006**, *38*, 68.
(15) Kocoglu, M. E.; Bayram, A.; Balci, I. *J. Microbiol.* **2005**, *43*, 257.
(16) Osawa, K.; Nakajima, M.; Kataoka, N.; Arakawa, S.; Kamidono, S. *J. Infect. Chemother.* **2002**, *8*, 353.
(17) O'Toole, R.; Kolter, G. A. *Mol. Microbiol.* **1998**, *30*, 295.
(18) Lequette, Y.; Greenberg, E. P. *J. Bacteriol.* **2005**, *187*, 37.
(19) Kirisits, M. J.; Parsek, M. R. *Cell. Microbiol.* **2006**, *8*, 1841.
(20) Ramsey, M. M.; Whiteley, M. *Mol. Microbiol.* **2004**, *53*, 1075.
(21) Hoyle, B. D.; Costerton, W. J. *Prog. Drug. Res.* **1991**, *37*, 91.
(22) Lawrence, J. R.; Delaquis, P. J.; Korber, D. R. *Microb. Ecol.* **1987**, *14*, 1.
(23) Dekkers, L. C.; van der Bij, A. J.; Mulders, I. H.; Phoelich, C. C.; Wentwoord, R. A.; Glandorf, D. C.; Wijffelman, C. A.; Lugtenberg, B. J. *Mol. Plant-Microbe Interact.* **1998**, *11*, 763.
(24) de Weert, S.; Vermeiren, H.; Mulders, I. H.; Kuiper, I.; Hendrickx, N.; Bloemberg, G. V.; Vanderleyden, J.; De Mot, R.; Lugtenberg, B. J. *Mol. Plant-Microbe Interact.* **2002**, *15*, 1173.
(25) Diaz, C.; Schilardi, P. L.; Salvarezza, R. C.; Fernández Lorenzo de Mele, M. *Langmuir* **2007**, *23*, 11206.
(26) Corti, C. W.; Holliday, R. J. *Mater. World* **2003**, *11*, 12.
(27) Azzaroni, O.; Fonticelli, M.; Benítez, G.; Schilardi, P. L.; Gago, R.; Caretti, I.; Vázquez, L.; Salvarezza, R. C. *Adv. Mater.* **2004**, *16*, 405.
(28) Schilardi, P. L.; Dip, P.; dos Santos Claro, P. C.; Benitez, G. A.; Fonticelli, M. H.; Azzaroni, O.; Salvarezza, R. C. *Chem. Eur. J.* **2006**, *12*, 38.
(29) Gallegos, A.; Mazzag, B.; Mogilner, A. *Bull. Math. Biol.* **2006**, *68*, 837.
(30) Harshey, R. M. *Annu. Rev. Microbiol.* **2003**, *57*, 249.
(31) Ben-Jacob, E.; Levine, H. *J. R. Soc. Interface* **2006**, *3*, 197.
(32) Yarwood, J. M.; Bartels, D. J.; Volper, E. M.; Greenberg, E. P. *J. Bacteriol.* **2004**, *186*, 1838.

AM8000677